Medicine®

OBSERVATIONAL STUDY

OPEN

# Tumor Vascular Permeability Pattern Is Associated With Complete Response in Immunocompetent Patients With Newly Diagnosed Primary Central Nervous System Lymphoma

## *Retrospective Cohort Study*

*Sae Rom Chung, MD, Young Jun Choi, MD, Ho Sung Kim, MD, PhD, Ji Eun Park, MD, Woo Hyun Shim, PhD, and Sang Joon Kim, MD, PhD*

**Abstract:** A dynamic contrast-enhanced MR imaging (DCE-MRI) could provide the information about tumor drug delivery efficacy. We investigated the potential utility of the permeability pattern of DCE-MRI for predicting tumor response to high dose-methotrexate treatment and progression-free survival (PFS) in patients with primary CNS lymphoma (PCNSL). Clinical and conventional imaging parameters were assessed as potential predictors of tumor response in 48 immunocompetent PCNSL patients in a preliminary study. Fifty additional immunocompetent patients (27 men and 23 women; mean age, 60.6 years) with PCNSL underwent DCE-MRI before starting first-line treatment with high dose-methotrexate. The DCE-MRI pattern was categorized as diffuse or nondiffuse. After 4 courses of high dose methotrexate, patients underwent follow-up brain MR imaging to identify their complete response (CR). Predictors of CR and PFS were analyzed using clinical parameters, conventional MRI, and DCE-MRI. CR was noted in 20 (74.1%) of 27 patients with diffuse DCE-MRI pattern and in 4 (17.4%) of 23 patients with nondiffuse DCE-MRI pattern. The diffuse DCE-MRI pattern showed a significantly higher association with CR than the nondiffuse pattern ($P < 0.001$). Multivariate Cox proportional hazards model revealed that the DCE-MRI pattern (hazard ratio = 0.70; $P = 0.045$), age (hazard ratio = 1.47; $P = 0.041$), and adjuvant autologous stem-cell transplantation (hazard ratio = 6.97; $P = 0.003$) tended to be associated with a PFS. The pretreatment diffuse DCE-MRI pattern can be used as a potential imaging biomarker for predicting CR and a longer PFS in patients with newly diagnosed PCNSLs.

Editor: Yong Liu.
Received: October 6, 2015; revised: January 2, 2016; accepted: January 5, 2016.
From the Department of Radiology and Research Institute of Radiology, University of Ulsan College of Medicine, Asan Medical Center, Seoul, Korea.
Correspondence: Ho Sung Kim, Department of Radiology and Research Institute of Radiology, University of Ulsan College of Medicine, Asan Medical Center, 86 Asanbyeongwon-Gil, Songpa-Gu, Seoul 138-736, Korea (e-mail: radhskim@gmail.com).
SRC and YJC are co-first authors and equally contributed to this paper.
This study was supported by a grant (2014-0368) from the Asan Institute for Life Sciences, Asan Medical Center, Seoul, Korea.
The authors have no conflicts of interest to disclose.

ISSN: 0025-7974
DOI: 10.1097/MD.0000000000002624

(*Medicine* 95(6):e2624)

**Abbreviations**: BBb = lood–brain barrier, CR = complete response, DCE-MRI = dynamic contrast-enhanced magnetic resonance imaging, DSC = dynamic susceptibility contrast, DWI = diffusion-weighted imaging, PCNSL = primary central nervous system lymphoma, PD = progressive disease, PET = positron emission tomography, PFS = progression-free survival, PR = partial response, SD = stable disease, WBRT = whole-brain radiotherapy.

## INTRODUCTION

Since the response to induction methotrexate therapy was reported to be a strong predictor of both prognosis and survival in several studies,[1,2] the ability to predict the initial tumor response may be potentially helpful in triaging the nonresponsive tumors to alternative strategies such as radiation or chemotherapy dose adjustment. Despite the concomitant risk of neurological toxicity, methotrexate-based chemotherapy requires high doses because of poor drug delivery across the blood–brain barrier (BBB).[3] Moreover, methotrexate-based chemotherapy potentiated by BBB disruption has shown promising results in primary central nervous system lymphoma (PCNSL) treatment.[4] Therefore, pretreatment direct or indirect assessment of drug delivery to brain tumors could be potentially useful for predicting initial treatment responses and devising strategies for reducing or increasing the dose of chemotherapeutic drugs.

It is well known that the response of a tumor to chemotherapy is primarily determined by the delivery of drugs to the tumor, and drug delivery depends on the vascular system of the tumor.[5] Therefore, imaging parameters associated with tumor vascular permeability patterns might be used as potential biomarkers of treatment responses in PCNSL. Thus, a tumor vascular pattern indicating maximum drug delivery can potentially reduce chemotherapeutic drug dose and minimize neurological toxicity.[3] Moreover, the availability of such a prognostic biomarker could contribute significantly to the selection of the most effective chemotherapeutic regimen, particularly in the case of monoclonal antibody therapy, which is less permeable through the BBB, but is reported to be more effective in PCNSL than current novel chemotherapeutic regimens.[4]

To monitor functional and structural changes in tumor vascularity followed by chemotherapy, various imaging modalities have been developed including dynamic contrast-enhanced computed tomography,[6,7] positron emission tomography (PET),[7,8] and dynamic contrast-enhanced magnetic

resonance imaging (DCE-MRI).[8,9] Among them, DCE-MRI has some advantages in terms of monitoring drug delivery compared with other imaging modalities. Theoretically, DCE-MRI-derived pharmacokinetic or model-free parameters could permit evaluation of tumor drug delivery, thereby allowing the assessment of therapeutic response to chemotherapeutic drugs. DCE-MRI has also been reported to be useful as an imaging biomarker of treatment response in liver cancer using the area under the time–concentration curve, suggesting perfusion was associated with higher response rates and longer survival.[10] Additionally, since DCE-MRI is more sensitive to small-vessel function than other modalities,[11] DCE-MRI techniques are adequate noninvasive methods to assess tumor vasculature and are accepted surrogate markers of tumor angiogenesis.[12]

Our institute treated all patients using high-dose methotrexate alone for tumors initially diagnosed as PCNSL, and then assessed response according to the International PCNSL Collaborative Group criteria. Additional treatment with chemotherapy including cytarabine or chemoradiation was indicated based on tumor response. Since DCE-MRI reflects the tumor microvascular environment and is a surrogate marker of drug delivery, we hypothesized that DCE-MRI may predict the treatment response to chemotherapy and can thus be proposed as a noninvasive biomarker for predicting the prognosis of patients with PCNSL. Therefore, our study was conducted to investigate the potential utility of the permeability pattern of DCE-MRI for predicting the complete response (CR) to high-dose methotrexate and progression-free survival (PFS) in patients with PCNSL.

## METHODS

### Study Design

The study protocols were approved by our institutional review board and informed consent from the study patients was waived due to the retrospective design of this study. From January 2006 to December 2010, clinical and conventional imaging parameters, including patient age, tumor location, laboratory findings, patient performance, and adjuvant treatment method, were initially assessed as potential predictors of early tumor response to high-dose methotrexate treatment and PFS in 48 PCNSL patients satisfying the following inclusion and exclusion criteria. All patients were diagnosed by stereotactic biopsy as having diffuse large B-cell lymphoma. All of these patients underwent baseline clinical and laboratory evaluations, including brain MRI, ophthalmologic consultation with slit-lamp examination, neck, chest and abdominal CT scans, and laboratory tests including HIV-1 serology. Patients lacking histological confirmation or follow-up visits were excluded. Also excluded were immune-compromised patients with HIV positivity and patients with systemic lymphoma that had spread to the brain. From the patients who met the inclusion criteria, significant predictors of CR and PFS were selected as confounders for the following DCE-MRI study.

From January 2011 to October 2015, DCE-MRI was used as a potential predictor of early tumor response to high-dose methotrexate treatment and PFS in PCNSL patients. During this period, 97 patients were diagnosed with PCNSL. The same inclusion and exclusion criteria were applied as in the previous clinical and conventional imaging parameter studies. Of the 97 patients, 25 who did not have any DCE-MRI data were excluded. Two patients with no histologic confirmation, 3 patients who underwent mass resection surgery, 6 patients with no follow-up imaging, 8 patients with secondary CNS lymphoma, and 3 patients who did not undergo initial high-dose methotrexate monotherapy were also excluded. Finally, 50 patients were enrolled in our DCE-MRI study, and referred to as ''study patients.'' Figure 1 summarizes the accrual process of the study population. Of the 50 study patients, 27 were man (mean age, 56.5 years; range, 29–77 years) and 23 were woman (mean age, 65.5 years; range, 51–76 years), and their overall mean age was 60.6 years (range, 29–77 years). The clinical and radiological characteristics of the study patients are summarized in Table 1.

### Treatment Protocol and Response Assessment

Our study patients diagnosed with PCNSL were first treated with 4 courses of high-dose methotrexate (3.5 mg/m$^2$ over 2 hours [maximum 7 g]) at 2-week intervals. There was no patient enrolled in this DCE-MRI study who received other

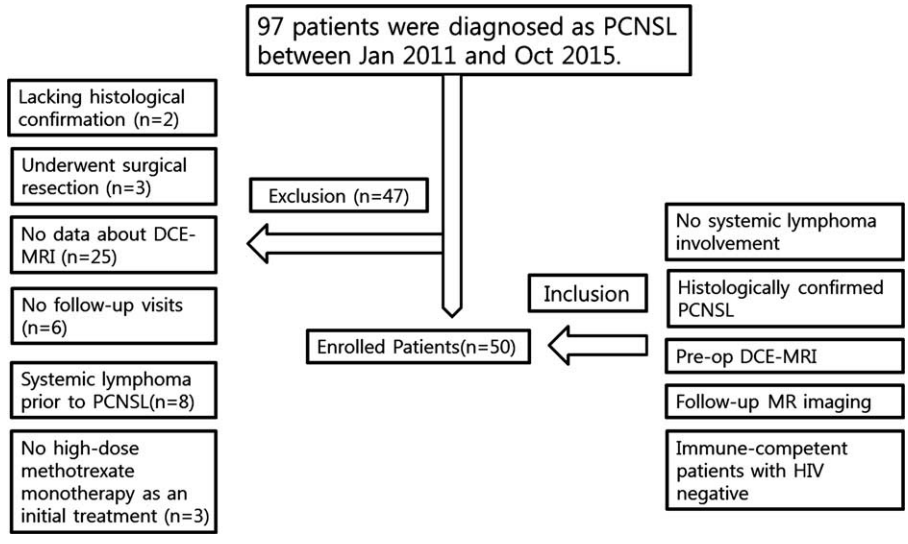


**FIGURE 1.** Flowchart of the study population. DCE-MRI = dynamic contrast-enhanced magnetic resonance imaging; PCNSL = primary central nervous system lymphoma; WBRT = whole brain radiotherapy.

**TABLE 1.** Summary of Clinical Data

| Variables | Diffuse Pattern (n = 27) | Nondiffuse Pattern (n = 23) | *P* Value |
|---|---|---|---|
| Age | | | 0.964 |
| < 60 yr | 13 (48.1 %) | 10 (43.5 %) | |
| ≥ 60 yr | 14 (51.9 %) | 13 (56.5 %) | |
| Sex | | | 0.539 |
| Male | 13 (48.1 %) | 14 (60.1 %) | |
| Female | 14 (51.9 %) | 9 (39.9 %) | |
| ECOG performance status | | | 0.430 |
| ≤ 1 | 10 (37.0 %) | 11 (47.8 %) | |
| ≥ 2 | 17 (63.0 %) | 12 (52.2 %) | |
| Conventional imaging findings | | | |
| Multiple | 13 (48.1 %) | 12 (52.2 %) | 0.992 |
| Necrosis | 2 (7.4 %) | 4 (17.4 %) | 0.087 |
| Hemorrhage | 0 (0 %) | 3 (13.0 %) | 0.102 |
| Meningeal involvement | 2 (7.4 %) | 2 (8.7 %) | 1.00 |
| Deep brain involvement | 17 (63.0 %) | 17 (73.9 %) | 0.601 |
| Mean total methotrexate dose, mg/m$^2$ | 21.2 ± 3.7 | 21.7 ± 3.8 | 0.649 |
| Mean time between pretreatment MRI and methotrexate, days | 14.4 ± 6.3 | 16.9 ± 9.5 | 0.069 |
| Mean time between methotrexate and follow-up MRI, days | 13.4 ± 4.3 | 14.6 ± 4.9 | 0.358 |
| EBV positivity | 5 (18.5 %) | 4 (17.4 %) | 0.790 |
| Mean serum LDH level | 189.1 ± 37.4 | 213.5 ± 65.3 | 0.145 |
| Mean CSF-total protein | 72.1 ± 43.5 | 105.2 ± 99.5 | 0.123 |
| Bcl-6 positivity | 18 (66.7 %) | 12 (52.2 %) | 0.452 |
| Autologous stem cell | 14 (51.9 %) | 13 (56.5 %) | 0.964 |
| Adjuvant radiation therapy | 4 (14.8 %) | 6 (26.1 %) | 0.523 |

ECOG = eastern cooperative oncology group, LDH = lactate dehydrogenase.

treatments in addition to high-dose methotrexate. A leucovorin rescue (30 mg q 6 hours) was started 24 hours after completion of high-dose methotrexate until a methotrexate level of 0.1 μmol/L was reached. Tumor response was assessed within 2 weeks following the initial high-dose methotrexate treatment using the International PCNSL Collaborative Group criteria, based on imaging, corticosteroid use, cerebrospinal fluid cytology, and slit-lamp examination in cases of cerebrospinal fluid or ocular involvement.[13]

Imaging analysis of the response was performed based on gadolinium-enhanced, T1-weighted imaging and diffusion-weighted imaging (DWI). The scans were analyzed by a clinically experienced, board-certified neuroradiologist (HSK, with 11 years of clinical experience in neurooncologic imaging). Patients who achieved CR or partial response (PR) after 4 courses of high-dose methotrexate were further treated with high-dose methotrexate (same regimen as mentioned above) with high-dose cytarabine (3000 mg/m$^2$ over 2 hours). The patients then underwent autologous stem cell transplantation, observation, or salvage treatment including chemotherapy and whole-brain radiotherapy (WBRT), according to the patient's age and residual lesion. Patients with stable disease (SD) or progressive disease (PD) were offered salvage therapy including WBRT and other chemotherapy regimens.

## Imaging Protocol

MR imaging studies were performed using a 3-T system (Achieva; Philips Medical Systems, Best, The Netherlands) with an 8-channel sensitivity-encoding head coil. Since May 2010, our brain tumor MRI protocol has included transverse T2-weighted fast-spin-echo imaging, transverse T1-weighted spin-echo imaging, DWI, DCE-MRI, contrast-enhanced transverse, sagittal, and coronal T1-weighted spin-echo imaging, and dynamic susceptibility contrast (DSC) perfusion MR imaging.

DCE-MRIs were performed using 3D gradient-echo data with 21 sections obtained before, during, and after administration of a standard dose of 0.1 mmol (0.2 mL)/kg of gadoteratemeglumine (Dotarem; Guerbet, Aulnay-sous-Bois, France) per kilogram of patient body weight (average total volume, 13.7 mL; range, 12–15 mL) and at a rate of 4 mL/s using an MR imaging–compatible power injector (Spectris; Medrad, Indianola, PA). The dynamic acquisition was performed with a temporal resolution of 3.52 seconds, and contrast was administered after 10 baseline dynamics (total, 120 dynamics).

## Image Processing and Analysis

All imaging data were transferred from the MRI scanner to an independent personal computer for semiquantitative DCE-MRI pattern analysis using a dedicated software package (Nordic ICE; NordicNeuroLab, Bergen, Norway). For DCE-MRI pattern analysis, we chose the model-free parameter since we focused only on the permeability pattern without quantitative value and our desire was to minimize the dependence on complex pharmacokinetic modeling which can be sensitive to noise. For the correction of interindividual variation, the signal intensity (SI) was normalized to the baseline SI value. We calculated the trapezoidal integration of the normalized SI with time over the first 30 seconds after postcontrast agent arrival in the enhancing voxels of interest, as described in a previously published study.[14] Outlier values that occurred due to unstable

curve fitting conditions with noisy input signals were automatically removed from the output maps.

All MRI scans were read by an experienced neuroradiologist (HSK) who was blinded to the clinical outcomes. Conventional MRI parameters included deep or superficial location, multiplicity, necrosis or hemorrhage component, and meningeal disease were also evaluated. Deep location means involvement of basal ganglia, corpus callosum, periventricular areas, brain stem, and cerebellum. Superficial location means involvement of the cerebral hemisphere, except the deep brain structure. The extent of the tumor was assessed by its largest diameter in 3 reformatted planes, for example, sagittal, axial, and coronal, based on contrast-enhanced T1-weighted images.

The DCE-MRI patterns were categorized into 2 types: a diffuse pattern characterized by a single spot of homogeneously increased permeability from the center to the periphery, resembling a centrifugal pattern within the corresponding contrast-enhancing lesion; and a nondiffuse pattern characterized by multifocal bright spots resulting in heterogeneously increased permeability pattern or by poor permeability within the corresponding contrast-enhancing lesion. Examples of DCE-MRI patterns are shown in Figure 2.

## Statistical Analysis

The primary endpoint was initial tumor response following high-dose methotrexate treatment. Patients were categorized into 4 groups according to their initial response: CR, PR, SD, and PD. Since our hypothesis was that a diffuse DCE-MRI pattern may be highly associated with CR, we dichotomized the initial tumor response into 2 groups, CR and non-CR, in the statistical analyses. We used multivariate logistic regression analysis, area under the receiver operating characteristic (ROC) curve (AUC) analysis, and cross validation to investigate the association between the CR rate and clinical and imaging parameters, including patient age, tumor location, laboratory findings, patient performance, and DCE-MRI pattern.

The secondary endpoint was PFS calculated from the initiation of chemotherapy until the first tumor progression or date of the last follow-up for patients without any event (censored data). Potential prognostic factors of PFS were compared using univariate and multivariate analyses. Univariate analysis was performed using the Kaplan–Meier method. To investigate the prognostic impact of DCE-MRI patterns on PFS, we used the multivariate Cox proportional hazard model.

Results were considered statistically significant at the 2-sided 5% comparison-wise significance level ($P < 0.05$). All statistical analyses were performed using SPSS version 21.0 (SPSS Inc, Chicago, IL) and R version R 2.15.3 (R Project for Statistical Computing, http://www.r-project.org).

# RESULTS

## Patient Characteristics

All of the study patients underwent initial treatment with high-dose methotrexate alone. The mean dose of methotrexate was 21.4 mg, the mean duration between pretreatment MRI and chemotherapy was 15.6 days, and 13.9 days elapsed between chemotherapy and the first post-treatment MRI. No patient died from treatment-related toxicity.

## Selection of Clinical and Conventional MR Imaging Parameters as Confounders

Table 2 shows the multivariate logistic regression conducted to test the predictive performance of the clinical and conventional imaging parameters in the 48 PCNSL patients from our preliminary study. The highest AUC value was noted for deep tumor location and was significantly associated with CR (odds ratio = 0.05; $P = 0.007$). Patient age (≥60 years),

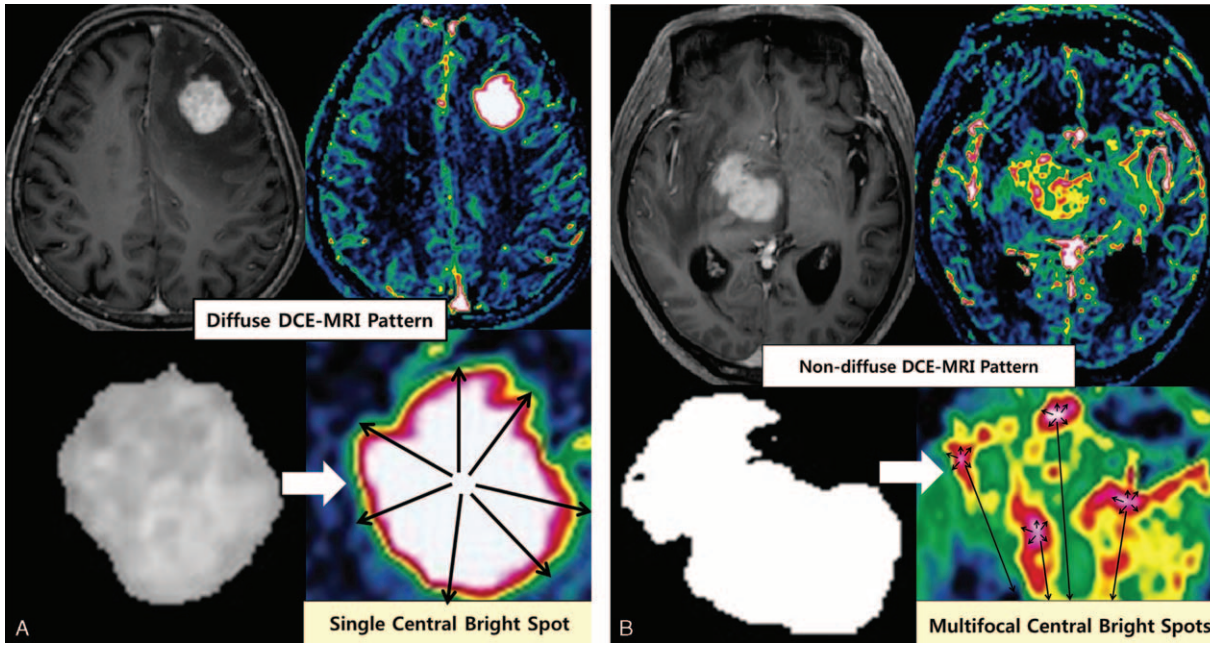


**FIGURE 2.** Examples of DCE-MRI Patterns. A, Diffuse and centrifugal bright spot of increased permeability at the corresponding contrast-enhancing lesion, classified as diffuse pattern. B, Multifocal centrifugal bright spots of increased permeability at the corresponding contrast-enhancing lesion, classified as nondiffuse pattern.

**TABLE 2.** Clinical and Conventional Imaging Parameters as Complete Response Predictors in 48 Patients With Primary CNS Lymphoma (Preliminary Study)

| Parameters | Odds Ratio | 95% CI of Odds Ratio | *P* Value | AUC |
|---|---|---|---|---|
| Age (≥60 yr) | 0.39 | 0.06–2.34 | 0.301 | 0.56 |
| Deep tumor location | 0.05 | 0.009–0.42 | 0.007 | 0.72 |
| LDH | 1.00 | 0.97–1.02 | 0.738 | 0.58 |
| ECOG performance (≤ 1) | 6.96 | 1.08–45.69 | 0.40 | 0.63 |
| CSF protein | 1.00 | 0.99–1.01 | 0.69 | 0.56 |

AUC = area under the receiver operating characteristic curve, CI = confidence interval, ECOG = eastern cooperative oncology group, LDH = lactate dehydrogenase.

LDH, patient performance, and CSF protein were not significant predictors for CR following high-dose methotrexate treatment in our preliminary study.

Table 3 shows the multivariate Cox proportional hazard model of the clinical and conventional imaging parameters for predicting PFS in the 48 PCNSL patients from our preliminary study. Patient age (≥60 years) (hazard ratio = 2.38; $P = 0.048$) and poor patient performance (hazard ratio = 2.63; $P = 0.047$) were significant predictors of shorter PFS; however, deep tumor location, LDH, patient performance, and CSF protein were not significant predictors of PFS in our preliminary study.

## DCE-MRI as a Predictor of CR After High-Dose Methotrexate Treatment

For the visual assessment of DCE-MRI, 27 patients showed diffuse patterns of permeability and 23 patients showed nondiffuse patterns. Since deep tumor location was only a significant parameter for predicting CR in the preliminary study, the DCE-MRI pattern was assessed as a potential CR predictor using a multivariate logistic regression model with deep tumor location as a confounder.

After the first high-dose methotrexate treatment, CR was noted in 20 (74.1%) of 27 patients with diffuse DCE-MRI patterns and in 4 (17.4%) of 23 patients with nondiffuse DCE-MRI patterns. The diffuse DCE-MRI pattern showed a significantly higher rate of CR than the nondiffuse pattern ($P < 0.001$) (Table 4). The results of the multivariate logistic regression showed a significant relationship between the DCE-MRI pattern and the CR rate (odds ratio = 32.93; $P = 0.002$) (Table 5). The deep tumor location also showed a significant relationship with the CR rate (odds ratio = 0.04; $P = 0.006$) (Table 5).

By ROC curve analysis, the DCE-MRI pattern showed a higher AUC than deep tumor location for predicting CR following the first high-dose methotrexate treatment; the cross-validation results revealed the same trend. The representative cases for the association of DCE-MRI pattern with initial tumor response are shown in Figures 3 to 5.

## DCE-MRI as a Predictor of PFS

Patient age was only a significant parameter for predicting PFS in the preliminary study, and recently, autologous stem cell

**TABLE 3.** Clinical and Conventional Imaging Parameters as Progression-Free Survival Predictors in 48 Patients With Primary CNS Lymphoma (Preliminary Study)

| Parameters | Hazard Ratio | 95% CI of Hazard Ratio | *P* Value of Hazard Ratio |
|---|---|---|---|
| Age (≥ 60 yr) | 2.38 | 1.02–5.55 | 0.043 |
| Deep tumor location | 0.72 | 0.30–1.72 | 0.46 |
| LDH | 1.00 | 0.99–1.01 | 0.49 |
| ECOG performance (≤ 1) | 2.63 | 1.03–6.27 | 0.047 |
| CSF protein | 0.99 | 0.99–1.01 | 0.45 |

CI = confidence interval, ECOG = eastern cooperative oncology group, LDH = lactate dehydrogenase.

**TABLE 4.** Association Between DCE-MRI Pattern and Tumor Response Pattern in the Study Population

| Outcome | Diffuse Pattern (n = 27) | Nondiffuse Pattern (n = 23) | *P* Value |
|---|---|---|---|
| Tumor response | | | <0.001 |
| Complete response | 20 (74.1%) | 4 (17.4%) | |
| Partial response | 7 (25.9%) | 19 (82.6%) | |
| Stable | 0 (0%) | 0 (0%) | |
| Progression | 0 (0%) | 2 (8.7%) | |

**TABLE 5.** Diagnostic Performance of DCE-MRI Pattern and Tumor Location as Complete Response Predictors in the Study Population

| Statistics | Deep Tumor Location | Diffuse DCE-MRI Pattern |
|---|---|---|
| Odds ratio | 0.04 | 32.93 |
| 95% CI of odds ratio | 0.004–0.40 | 3.78–287.15 |
| *P* value of odds ratio | 0.006 | 0.002 |
| AUC | 0.71 | 0.78 |
| 95% CI of AUC | 0.57–0.83 | 0.64–0.89 |
| Cross-validated AUC | 0.70 | 0.77 |
| Cross-validated accuracy | 73.7% | 79.5% |

AUC = area under the receiver operating characteristic curve, CI = confidence interval.

transplantation has been used as an adjuvant to high-dose methotrexate at our institution. Therefore, the DCE-MRI pattern was assessed as a potential PFS predictor using a multivariate Cox proportional hazard model with patient age and autologous stem cell transplantation as confounders.

Using the entire study population, 37 (74.0%) patients experienced a recurrence during the follow-up period (range, 9–35.2 months). The median PFS was 27.1 months (95% confidence interval, 23.0–29.1 months). In subgroup analysis, a recurrence was noted in 18 (85.7%) of 27 patients with diffuse DCE-MRI patterns and in 19 (82.6%) of 23 patients with nondiffuse DCE-MRI patterns. The median PFS was 27.8 months (95% confidence interval, 25.0–30.1 months) in the diffuse DCE-MRI group and 26.1 months (95% confidence interval, 9.7–27.3 months) in the nondiffuse DCE-MRI group (Figure 6).

The results of the multivariate Cox proportional hazard model are summarized in Table 6. The multivariate Cox proportional hazard model revealed that DCE-MRI pattern (hazard ratio = 0.70; $P = 0.045$), age (hazard ratio = 1.47; $P = 0.041$), and adjuvant autologous stem cell transplantation (hazard ratio = 6.97; $P = 0.003$) tended to be associated with PFS.

## DISCUSSION

In this study, we investigated the power of pretreatment DCE-MRI patterns in predicting CR to high-dose methotrexate and PFS in PCNSL patients. Our results showed that diffuse DCE-MRI patterns were significantly associated with a higher CR rate after initial high-dose methotrexate than nondiffuse DCE-MRI patterns. Therefore, the assessment of BBB disruption by DCE-MRI may be associated with the extent of chemotherapeutic drug delivery to the PCNSL. Our results also showed that a diffuse DCE-MRI pattern tended to indicate a

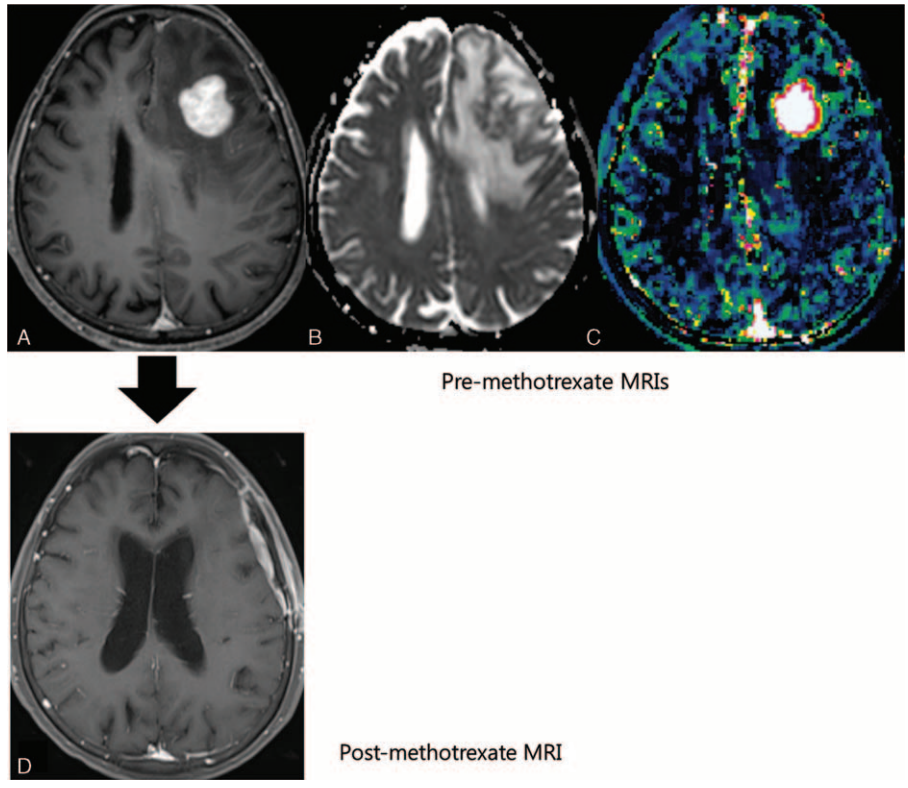


**FIGURE 3.** An example of diffuse DCE-MRI Pattern. Pre- and post-treatment images obtained in a 76-year-old woman with PCNSL. The contrast-enhanced T1-weighted imaging shows a homogeneously enhancing mass (A) with low apparent diffusion coefficient (B) in the left frontal lobe. The mass shows a diffuse DCE-MRI pattern in the corresponding contrast-enhancing lesion (C). After 4 cycles of high-dose methotrexate, contrast-enhanced T1-weighted imaging shows that the enhancing tumor has completely disappeared, thus indicating complete response (D).

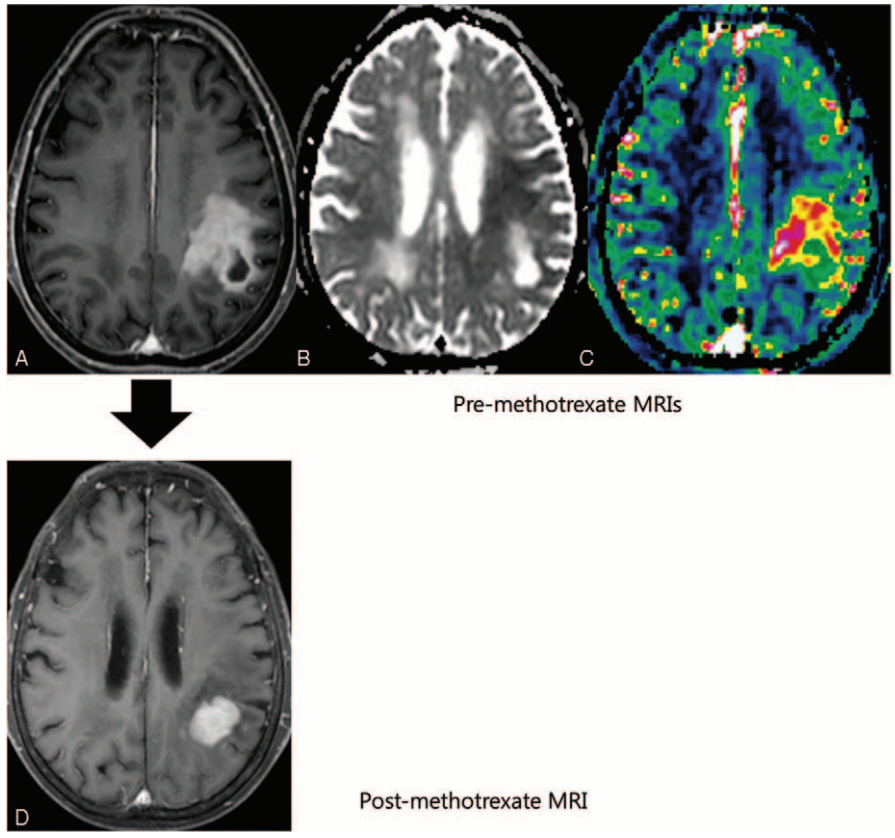


**FIGURE 4.** An example of nondiffuse DCE-MRI pattern. Pre- and post-treatment images obtained in a 72-year-old man with PCNSL. The contrast-enhanced T1-weighted imaging shows a relatively homogeneously enhancing mass except for a small nonenhancing portion (A) with low apparent diffusion coefficient (B) in the left parietal lobe. The mass shows a nondiffuse DCE-MRI pattern in the corresponding contrast-enhancing lesion (C). After 4 cycles of high-dose methotrexate treatment, contrast-enhanced T1-weighted imaging shows residual enhancing mass, thus indicating partial response (D).

longer PFS, although this result reached only borderline significance. These findings suggest that the pretreatment DCE-MRI pattern could be used as a potential noninvasive imaging biomarker for predicting the initial therapeutic response and prognosis in patients with PCNSL. In our study, initial uniform treatment with high-dose methotrexate and follow-up MRI studies on a regular schedule permitted the objective assessment of the relationship between the DCE-MRI pattern and the initial tumor response.

Given the importance of drug delivery to treatment efficacy, the ability to provide information on tumor microvasculature emphasizes a potential role of DCE-MRI in predicting initial therapeutic responses for chemosensitive tumor including PCNSL. The role of DCE-MRI for chemotherapeutic monitoring has been reported in many extracranial solid tumors.[15,16] Another previous report showed that the pretreatment DCE-MRI could also provide the information about tumor treatment response in breast cancer.[17] Recently, in intrahepatic cholangiocarcinoma treated with hepatic artery infusion, pretreatment DCE-MRI might help identify the patients who will benefit the most from hepatic arterial infusion.[18] However, perfusion-related enhanced drug delivery may not be the only factor underlying drug efficacy since the mechanism of action of chemotherapeutic drugs varies significantly with tumor type.[19] A recent study of DCE-MRI in patients with colorectal liver metastases undergoing 5-FU treatment reported that $K_{trans}$ measured before treatment did not predict treatment response.[19] These results suggest that the predictive value of the pretreatment parameters of DCE-MRI may depend on the tumor type studied, the kind of chemotherapy administered, and the paramagnetic contrast agent employed.[19] This is why we elected to study PCNSL, which is reported to be chemosensitive.

During the angiogenic process, as the tumor grows, blood vessels are often dilated and have branching patterns with excessive loops and arterio-venous shunts.[20] The walls of tumor vessels show lack or destruction of basement membranes, and fewer pericytes and may also lack perivascular smooth muscle.[21] As tumor vascular structures become progressively more disorganized, the resistance to blood flow increases. As a result, the blood supply to the tumor is impaired, and the delivery of nutrient metabolites and clearance of metabolic breakdown products are inefficient. The delivery of anticancer drugs is similarly compromised.[22] Since DCE-MRI can reflect tumor vascularity and permeability, a heterogeneous or poor perfusion pattern revealed by DCE-MRI consequently results in poor drug delivery to the tumor. This could explain why diffuse DCE-MRI patterns showed a higher rate of CR than nondiffuse patterns in our study.

No study has previously evaluated the value of DCE-MRI in predicting the prognosis of PCNSL. Currently, since brain MRI with a perfusion study is generally used as the initial

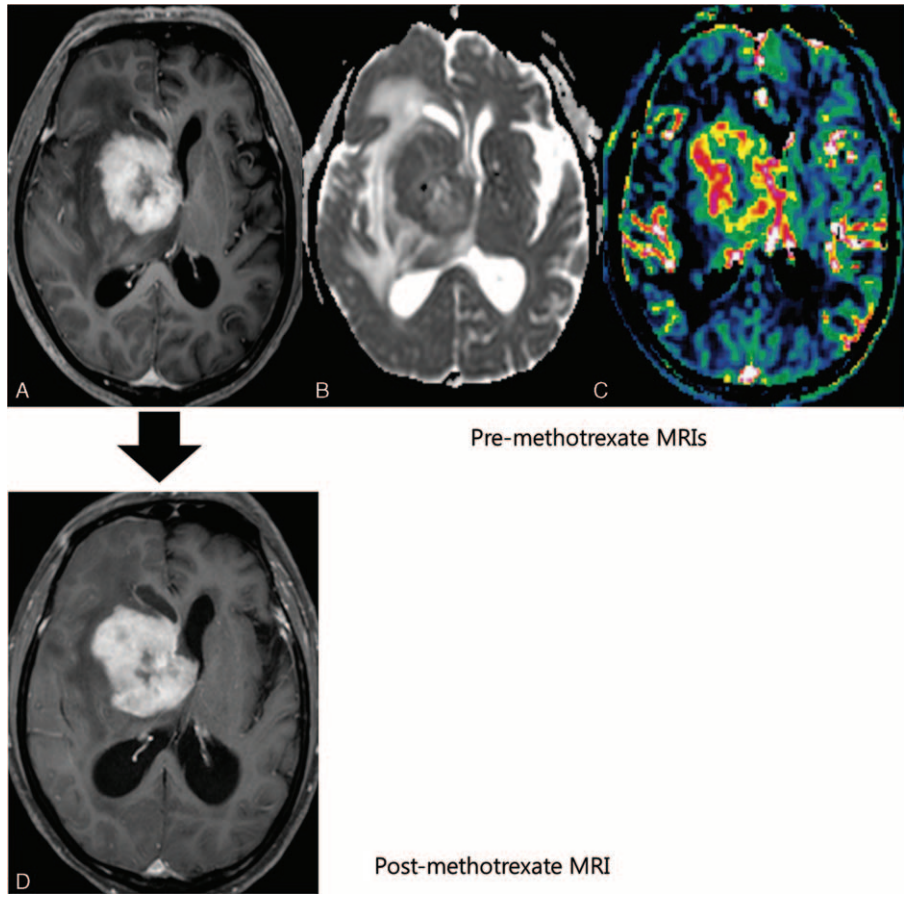


**FIGURE 5.** An example of nondiffuse DCE-MRI pattern. Pre- and post-treatment images obtained in a 67-year-old woman with PCNSL. The contrast-enhanced T1-weighted imaging shows a relatively homogeneously enhancing mass except for a central nonenhancing portion (A) with low apparent diffusion coefficient (B) in the right basal ganglia. The mass shows a nondiffuse DCE-MRI pattern in the corresponding contrast-enhancing lesion (C). After 4 cycles of high-dose methotrexate, contrast-enhanced T1-weighted imaging shows an enlarged enhancing mass, thus indicating progressive disease (D).

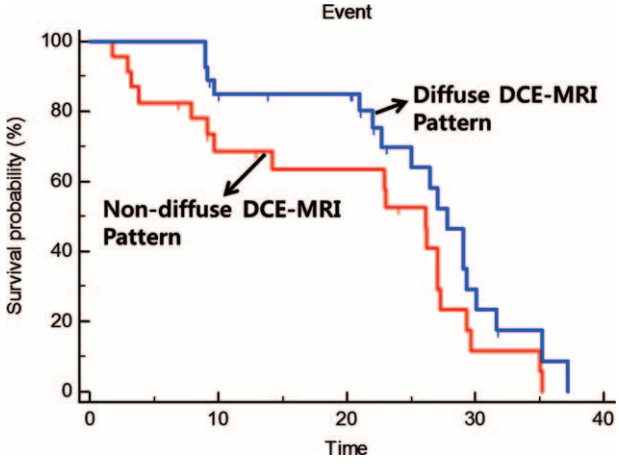


**FIGURE 6.** Comparison of progression-free survival curves between the diffuse DCE-MRI group and the nondiffuse DCE-MRI group.

evaluation tool for patients with a brain tumor, the pattern of DCE-MRI could be used as a readily available and effective biomarker. It is well known that the response to initial high-dose methotrexate therapy is significantly associated with better patient survival and prognosis.[1,2] By multivariate analysis, the diffuse DCE-MRI pattern, which was significantly associated with the rate of CR to the initial high-dose methotrexate therapy, was also associated with longer PFS, but with only borderline significance, perhaps because of the small sample size. Further studies with larger patient populations and long-term follow-up data are, therefore, warranted.

Our study has several limitations including small sample size due to the rarity of the disease, lack of long-term follow-up, lack of external validation, and retrospective design. In particular, the prognostic factors obtained in our study need to be validated in a larger, prospective trial to establish a prospective dataset to refine the present scores and establish new risk factors.

In conclusion, the data from this study show that pretreatment DCE-MRI may be a suitable noninvasive imaging biomarker of response to initial high-dose methotrexate and of prognosis in patients with PCNSL, with diffuse DCE-MRI patterns significantly associated with a higher rate of CR and also associated, although without any statistical significance,

**TABLE 6.** Clinical and Imaging Parameters as Progression-Free Survival Predictors in the Study Population

| Parameters | Hazard Ratio | 95% CI of Hazard Ratio | *P* Value of Hazard Ratio |
|---|---|---|---|
| Diffuse DCE-MRI pattern | 0.70 | 0.34–0.95 | 0.045 |
| Age (≥60 yr) | 1.47 | 1.05–8.61 | 0.041 |
| No autologous stem cell | 6.97 | 1.92–22.15 | 0.003 |

CI = confidence interval.

with longer PFS. Therefore, pretreatment DCE-MRI studies may have an important role to play, not only in diagnosis, but also in the establishment of prognosis in patients with newly diagnosed PCNSL.

## REFERENCES


1. McAllister LD, Doolittle ND, Guastadisegni PE, et al. Cognitive outcomes and long-term follow-up results after enhanced chemotherapy delivery for primary central nervous system lymphoma. *Neurosurgery.* 2000;46:51–60.
2. Momota H, Narita Y, Maeshima AM, et al. Prognostic value of immunohistochemical profile and response to high-dose methotrexate therapy in primary CNS lymphoma. *J Neurooncol.* 2010;98:341–348.
3. Jahnke K, Doolittle ND, Muldoon LL, et al. Implications of the blood-brain barrier in primary central nervous system lymphoma. *Neurosurg Focus.* 2006;21:E11.
4. Holdhoff M, Ambady P, Abdelaziz A, et al. High-dose methotrexate with or without rituximab in newly diagnosed primary CNS lymphoma. *Neurology.* 2014;83:235–239.
5. Goel S, Duda DG, Xu L, et al. Normalization of the vasculature for treatment of cancer and other diseases. *Physiol Rev.* 2011;91:1071–1121.
6. Rehman S, Jayson GC. Molecular imaging of antiangiogenic agents. *Oncologist.* 2005;10:92–103.
7. Cao M, Liang Y, Shen C, et al. Developing DCE-CT to quantify intra-tumor heterogeneity in breast tumors with differing angiogenic phenotype. *IEEE Trans Med Imaging.* 2009;28:861–871.
8. de Langen AJ, van den Boogaart VE, Marcus JT, et al. Use of H2(15)O-PET and DCE-MRI to measure tumor blood flow. *Oncologist.* 2008;13:631–644.
9. Taylor JS, Tofts PS, Port R, et al. MR imaging of tumor microcirculation: promise for the new millennium. *J Magn Reson Imaging.* 1999;10:903–907.
10. Jarnagin WR, Schwartz LH, Gultekin DH, et al. Regional chemotherapy for unresectable primary liver cancer: results of a phase II clinical trial and assessment of DCE-MRI as a biomarker of survival. *Ann Oncol.* 2009;20:1589–1595.
11. Yang X, Knopp MV. Quantifying tumor vascular heterogeneity with dynamic contrast-enhanced magnetic resonance imaging: a review. *J Biomed Biotechnol.* 2011;2011:732848.
12. Marzola P, Degrassi A, Calderan L, et al. In vivo assessment of antiangiogenic activity of SU6668 in an experimental colon carcinoma model. *Clin Cancer Res.* 2004;10:739–750.
13. Abrey LE, Batchelor TT, Ferreri AJ, et al. Report of an international workshop to standardize baseline evaluation and response criteria for primary CNS lymphoma. *J Clin Oncol.* 2005;23:5034–5043.
14. Chung WJ, Kim HS, Kim N, et al. Recurrent glioblastoma: optimum area under the curve method derived from dynamic contrast-enhanced T1-weighted perfusion MR imaging. *Radiology.* 2013;269:561–568.
15. Yamashita Y, Baba T, Baba Y, et al. Dynamic contrast-enhanced MR imaging of uterine cervical cancer: pharmacokinetic analysis with histopathologic correlation and its importance in predicting the outcome of radiation therapy. *Radiology.* 2000;216:803–809.
16. George ML, Dzik-Jurasz AS, Padhani AR, et al. Non-invasive methods of assessing angiogenesis and their value in predicting response to treatment in colorectal cancer. *Br J Surg.* 2001;88:1628–1636.
17. Chang YC, Huang CS, Liu YJ, et al. Angiogenic response of locally advanced breast cancer to neoadjuvant chemotherapy evaluated with parametric histogram from dynamic contrast-enhanced MRI. *Phys Med Biol.* 2004;49:3593–3602.
18. Konstantinidis IT, Do RK, Gultekin DH, et al. Regional chemotherapy for unresectable intrahepatic cholangiocarcinoma: a potential role for dynamic magnetic resonance imaging as an imaging biomarker and a survival update from two prospective clinical trials. *Ann Surg Oncol.* 2014;21:2675–2683.
19. van Laarhoven HW, Klomp DW, Rijpkema M, et al. Prediction of chemotherapeutic response of colorectal liver metastases with dynamic gadolinium-DTPA-enhanced MRI and localized 19F MRS pharmacokinetic studies of 5-fluorouracil. *NMR Biomed.* 2007;20:128–140.
20. Jain RK. Determinants of tumor blood flow: a review. *Cancer Res.* 1988;48:2641–2658.
21. Carmeliet P, Jain RK. Angiogenesis in cancer and other diseases. *Nature.* 2000;407:249–257.
22. Durand RE. Intermittent blood flow in solid tumours: an underappreciated source of 'drug resistance'. *Cancer Metastasis Rev.* 2001;20:57–61.